Evaluation of range error calibration models for indoor UWB positioning applications

Harris Perakis
School of Rural and Surveying Engineering
National Technical University of Athens (NTUA)
Athens, Greece
hperakis@central.ntua.gr

Vassilis Gikas
School of Rural and Surveying Engineering
National Technical University of Athens (NTUA)
Athens, Greece
vgikas@central.ntua.gr

***Abstract*— Recent improvements in the field of wireless technologies has led to an increase of available tools for Location Based Services (LBS). Modern indoor LBS applications continually raise the bar of requirements for the employed positioning technology and Ultra-Wide Band (UWB) ranging has become relevant by providing adequate performance. UWB employs modulated impulse signals for achieving ranging accuracies in the order of cm offering increased capabilities compared to other Radio-Frequency ranging methods. In order for the UWB systems to function reliably in complex indoor environments, error mitigation techniques are employed based on ranging error modelling methods. In this study, a commercial UWB system (Time Domain®) is employed for the development of error calibration models based on data collected in an indoor office environment. Three calibration methods are examined both for static and kinematic test scenarios. An overall improvement of 32%-86% is demonstrated for the static UWB ranges data while a 74% improvement on kinematic data results in a mean trajectory accuracy of 9 cm.**

Keywords—Ultra-Wide Band; RF ranging; calibration; range error modelling; indoor positioning

I. INTRODUCTION

The provision of continuous, accurate and ubiquitous positioning functionality becomes increasingly a key element for foreseen intelligent, wirelessly connected terminals. Currently, wireless positioning applications rely mostly on GNSS as it provides autonomous and global coverage with sufficient accuracy [1]. However, its working capability is limited to the outdoor environments that enable unobscured satellite tracking, while tree foliage and urban canyon conditions lead to the signal attenuation and multipath that deteriorate the positioning solution. [2]. For indoor positioning applications a wide range of localization techniques have been developed in recent years that employ sensor technologies ranging from optical to inertial and radio-based ones. In this regard, Pedestrian Dead reckoning (PDR) relies on inertial sensors due to their self-contained functionality [3]. Also, a large portion of current research focuses on map-matching techniques that utilize map information to compute geographical information that bounds the positioning solution [4]. Other, techniques employ the position lateration and fingerprinting principles to benefit Radiofrequency (RF) technologies such as Radio Frequency Identification (RFID), Wireless Local Area Network (WLAN) and Ultra-Wide Band (UWB) [5-7].

UWB technology is based on RF signal transmissions in the form of short pulses which results in the wide bandwidth of RF waveforms. The short nature of the emitting pulses provides range estimation of high accuracy via Time of Arrival techniques. The natural characteristics of UWB signal offer both Non-Line-of-Sight (NLOS) functionality and increased multipath resistance which are of great importance for complex indoor environments. Also, the signal transmission is performed at low power spectral densities resulting in low interference with other narrowband receivers while it prevents human body harmfulness [8]

Despite the resilient nature of UWB technology, the complex geometry and the varying conditions of indoor environments (pedestrians walking, furniture, etc.) consist a challenge for accurate UWB ranging. Common error sources include the dynamic multipath conditions along with the different structural materials and human body that UWB signals penetrate resulting to range measurements inconsistencies.

The main contributions of this paper include the evaluation of different UWB range calibration techniques based on a general methodology for implementing ad-hoc UWB calibration and the proposal of a weighting scheme for the ranging accuracy based on reported signal values. The rest of the paper is organized as follows. Section II summarizes the state of the art. The general UWB calibration methodology is described in section III. Section IV provides a description of the field-test and pre-processing, followed by the illustration of the calibration results in section V. Finally, a summary of the work and relevant suggestions is presented in section VI.

II. STATE OF THE ART

Extensive research is currently undertaken in many research centers worldwide to study the nature of RF ranging error sources and their impact on the positioning solution. Regarding RF range error modelling [9] proposes an asymmetric double exponential ranging error distribution model and an extension for range-defined model parameters

978-1-5386-5635-8/18/$31.00 ©2018 IEEE

tuning. In [10] a Ranging Quality Indicator (RQI) is established based on UWB signal characteristics paired with the corresponding ranging error in order to train a Machine Learning (ML) algorithm. In this approach, the ML algorithm produces a set of RQI values in real time and weighs accordingly the impact of the ranging data in a UWB/IMU particle filter collaborative positioning algorithm. In a study produced by [11] the original UWB ranges histograms produce multiple peaks due to multipath effects. To this effect, the Maximum Likelihood Estimator (MLE) is used for selecting the ranges with highest probability based on the lateration-generated coordinates. In a recent study published by [7] error calibration is performed using a grid of calibration points. In this approach the calibration values are used for the 2D linear interpolation forming the calibration function. In [12] a Sparse Pseudo-input Gaussian Process is trained using known relative antenna pose (angle) and error on fixed distances between UWB nodes. In this study the goal is to build an error prediction model for use in Kalman filtered based UWB positioning.

Regarding the field testing setups followed currently for UWB range error identification different approaches exist depending on the testing scope. For instance, [9] perform a series of static indoor field tests for estimating the range error values using multiple anchor nodes and mobiles. The area's concrete and steel walls result in predominantly NLOS conditions while the entire sets of data (LoS, multipath and NLoS) are analyzed together for the generation of error models providing improved positioning performance. In [7] tests are conducted at variant observation conditions – i.e., an outdoor open area, a forest environment and indoors. The different environment conditions indicate the varying effects on UWB positioning. Subsequently, the error calibration process is based on known calibration points forming a grid.

III. METHODOLOGY

A. *Statistical characterization of range errors*

At a first stage and before we apply any error range modeling the raw UWB measurements undergo through preliminary statistical analysis. For this purpose, a number of specifically designed experiments take place using an accurately surveyed testbed. Particularly, the exact location of the UWB nodes is selected so that the behavior of ranging errors is examined in a controlled environment. In this regard, the extracted statistical measures offer a description of the performance characteristics of UWB ranging leading to the next step of developing the data-driven range error models.

B. *Empirical range error models development*

For the development of range error models, it is essential that complete data-sets covering the total area of interest are collected. Prior to defining the error models, the data statistical metrics obtained in the previous step are evaluated in order to guide data grouping, data exclusion or further data collection. The error models are generated based on data-driven optimization techniques (e.g. best-fitting curves, interpolation) and are statistically evaluated before the implementation on real data for gross deviations identification, and data over-fitting.

C. *Error mitigation*

Error mitigating includes implementation of the developed error models on real ranging data. For the purpose of unbiased evaluation, the calibration is performed on data collected for validation purposes and not on the initial data collected for error modelling. The proposed range error models refer to disparate operational conditions (e.g. room type and geometry). This step provides the evaluation of the error models based on real, reference data.

D. *Kinematic positioning*

The final step of the methodology is the evaluation of the generated error models during kinematic positioning sessions. The dynamic character of the kinematic data provides the most demanding conditions for UWB range error model validation due to the varying environment. For validating the reliability and robustness of the models a set of test trajectories are build that cover the entire testbed area.

IV. FIELD TESTING AND PRE-PROCESSING

A. *Ranging equipement*

The UWB system used during field testing is the P410 module of Time Domain® which is based on coherent transmission of very short duration RF waveforms. The high resolution of the transmitted pulses offers the ability to perform high accuracy range measurements along with NLOS ranging and multipath rejection. Ranging is performed using the Two-Way Time of Flight technique (TW-ToF) in which the total travel time of the RF signal and the processing time of the UWB responder is multiplied by the RF signal velocity in order to obtain the Precise Range Measurement (PRM) value.

The high nominal ranging accuracy of the P410 module reported by the manufacture (~3cm for calibrated UWB pairs) relies on the ability of the transceivers to precisely identify the first received pulse also defined as Leading Edge Detection (LED) feature. This module along with ranging information is able to report the corresponding LED flag values that provide information about the ranging conditions (LOS, NLOS, Saturated: large amplitude due to short distance or high transmission power).

B. *Indoor laboratory test site*

The field test campaign took place indoors within the premises of the School of Rural and Surveying Engineering, NTUA. The laboratory area includes two separate office areas connected with a small corridor and a third smaller room offering the ability to collect UWB ranges both in LOS and NLOS conditions. Concerning range calibration evaluation, specific calibration and validation points were defined in order to cover the entire area in a uniform manner. Specifically,5 calibration points were established in Rooms 1 and 2 respectively and 1 calibration point in Room 3. Similarly,3 validation points were established in Rooms 1 and 2 respectively and 2 validation points in Room 3.

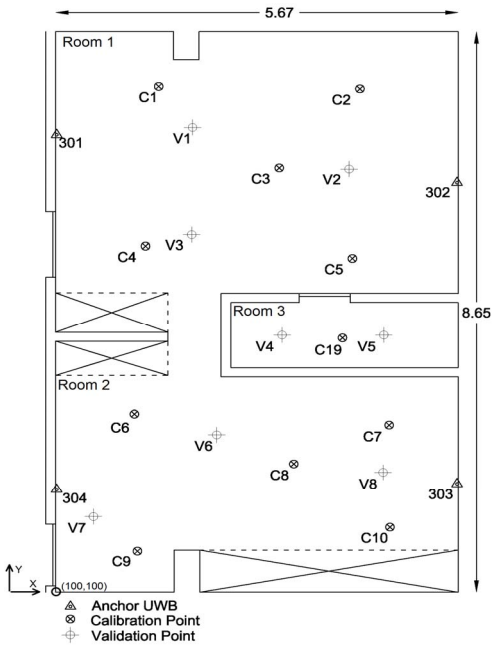

Fig. 1. Indoor laboratory top view showing the locations of the calibration, validation and anchor points

The complete test area is illustrated in Fig. 1 indicating the room IDs, the location of the calibration and validation points and the location of the 4 UWB anchor nodes. The UWB anchors nodes [301, 302, 303, 304] were installed on the surrounding walls of the laboratory [Fig. 2 (a)] with the goal of creating a symmetrical inter-nodal geometry for the needs of the field test. Prior to conducting the data collection sessions all the points were accurately surveyed in order to compute their coordinates in a local cartesian coordinate system with the lower-left corner of the laboratory set to 100,100. The axes orientation is illustrated in Fig. 1. For the collection of the calibration and validation points the mobile UWB node [300] was attached on a geodetic pole positioned vertically on each point of interest [Fig. 2 (b)] while lever-arms were measured before-hand.

(a) (b)

Fig. 2. Time Domain® UWB modules during field testing - anchor node attached on the wall (a), mobile node located at point C3 (b)

C. Calibration and validation range measurements

Data collection concerning the calibration and validation points employed a measuring pole located at each point while the mobile UWB node was connected to a data collection PC running a custom-built range collection Matlab® script. The mean ranging time is 30 s spanning approximately 150 range measurements (TW-TOF) per anchor node. The created logfile includes the measured range value, the estimated range error as produced by the UWB module, the recorded Leading-Edge Detection (LED) flag and the corresponding timestamps as illustrated in Fig. 3.

	A	B	C	D	E	F	G	H	I	J	K	L	M
1	Internal TimeStamp	ReqID	RspID	PRM(m)	PRMErr(m)	FRE(m)	FREErr(m)	CRE(m)	CREErr(m)	LED flags	PChour	PCminutes	PCseconds
2	407.113	300	301	1.782	0.055	1.782	0.065	1.782	0.055	9	14	8	36.041
3	407.129	300	302	4.461	0.055	4.461	0.065	4.461	0.055	9	14	8	36.076
4	407.144	300	303	7.634	0.024	7.634	0.034	7.634	0.024	8	14	8	36.092
5	285.802	301	302	5.801	0.055	NaN	NaN	NaN	NaN	9	14	8	36.107
6	285.817	301	303	8.359	0.056	NaN	NaN	NaN	NaN	8	14	8	36.128
7	3233.729	302	304	7.733	0.056	NaN	NaN	NaN	NaN	40	14	8	36.136
8	407.222	300	303	0	0	7.633	0.036	7.275	4.802	40	14	8	36.142
9	3233.869	302	303	5.424	10.536	NaN	NaN	NaN	NaN	56	14	8	36.163
10	274.227	303	304	5.711	0.055	NaN	NaN	NaN	NaN	9	14	8	36.194
11	407.284	300	302	4.461	0.055	4.461	0.058	4.461	0.055	9	14	8	36.21
12	407.3	300	303	7.673	0.055	7.667	0.058	7.673	0.055	8	14	8	36.23
13	407.316	300	304	6.861	0.056	6.853	0.059	6.861	0.056	40	14	8	36.238
14	285.833	301	304	6.021	0.129	NaN	NaN	NaN	NaN	16	14	8	36.245
15	285.957	301	302	5.801	0.055	NaN	NaN	NaN	NaN	9	14	8	36.264
16	285.957	301	302	5.801	0.055	NaN	NaN	NaN	NaN	9	14	8	36.284
17	3233.885	302	304	7.698	0.056	NaN	NaN	NaN	NaN	40	14	8	36.288
18	407.378	300	303	0	0	7.673	0.06	8.064	5.322	40	14	8	36.335

Fig. 3. Part of the ranges logfile collected during field testing

The histograms of Fig. 4 show the distribution of the range dataset collected for every pair of UWB nodes at calibration point C1. Freedman-Diaconis is used for optimizing the bin size selection [13]. From Fig. 4 is evident that the data do not follow a normal distribution suggesting that the selection for the best-fitting statistical value should be investigated.

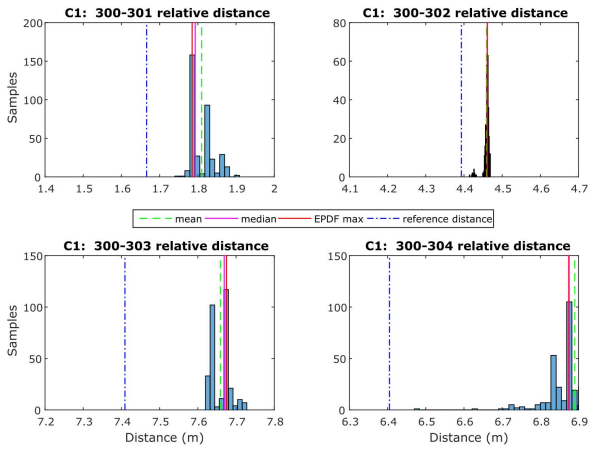

Fig. 4. Range histograms for all UWB node-pairs at point C1

The Empirical Probability Density Function is estimated using kernel density estimation with a kernel bandwidth value of 0.005 [14] resulting in a good fit for the P410 module UWB data. The range values used for further processing are the ones with the highest probability density (EPDF max) as the most representative of the samples. The necessity for a range

correction technique is obvious based on the offset of the depicted Reference distance values.

Fig. 5 depicts in red the range differences computed between the observed and reference values. Furthermore, the median LED flags are shown in blue along with the corresponding standard deviations for the different ranges. According to the manufacturer the LED flag value for LOS conditions should equal 8 whereas larger values indicate NLOS operation. Fig. 8 confirms this hypothesis. Also, a relation between the recorded LED values and the corresponding range deviations is observed indicating that the reported LED values can be utilized as an index for characterizing the ranges along with their reported range error values.

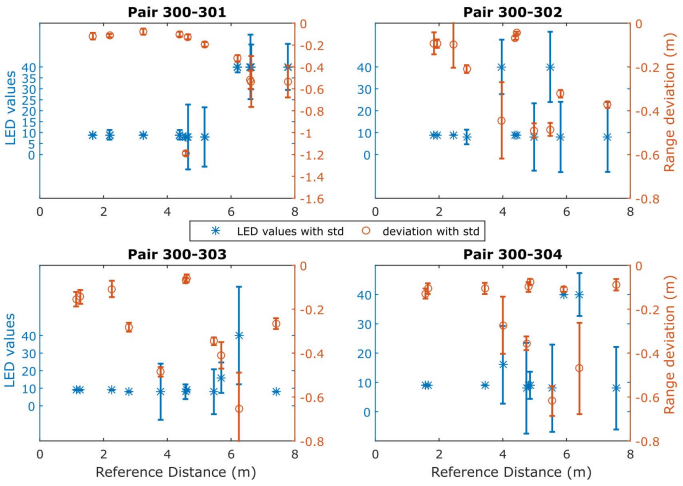

Fig. 5. LED flags with corresponding range deviations along with the standard deviation values for all UWB pairs

D. *Kinematic positioning session*

The last section of the field test includes the collection of the kinematic UWB ranges using a mobile node held by a pedestrian walking along a predefined travel path [C1→V1→C3→V2→C5→V3→V6→C6→C9→C8→C7→C10]. This travel path consists of low speed walking sections with short (~10 sec) stop & go parts when passing on points C1 to C10. The travel path traverses Room 1 and Room 2 via the short corridor. The total travel time of the kinematic trajectory is ~2.5 min while collecting a total of ~700 ranges per anchor node. The range timeseries collected during the kinematic session are illustrated in Fig. 6 showing an initial agreement between the aforementioned trajectory description and the reported range variations.

V. CALIBRATION AND RESULTS

A. *Range calibration*

Following previous studies, the calibration process concerning the P410 UWB modules could be based either on empirical radial corrections obtained by a least squares line fit to the range deviations as a function of the distance [14] or using a 2-dimensional range deviations plane fit [7]. In this study we examine both approaches in order to select the appropriate calibration technique that suits the collected data-set.

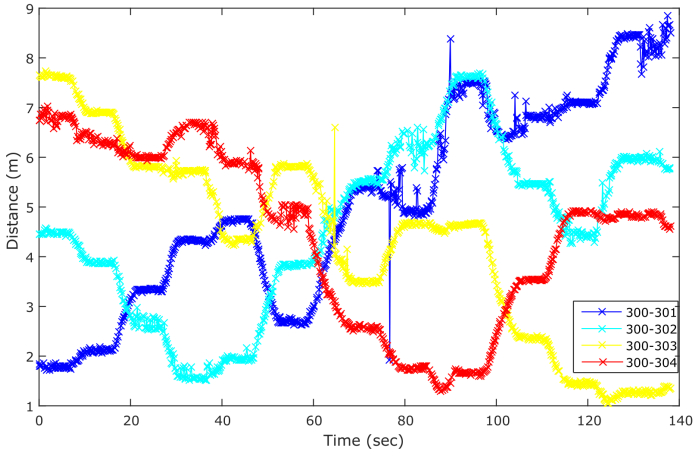

Fig. 6. Uncalibrated ranges timeseries for all UWB pairs during the kinematic session

For the case of radial calibration two different variations are considered based on the distribution of the calibration points in the corresponding rooms. The first variation known as "RoomLinearCal" produces a linear approximation of the calibration values for each room as dictated by the constant LOS or NLOS ranging conditions to specific anchor nodes each time. In essence, the calibration model for Room 1 corresponds to only LOS ranging for anchors 301 and 302 while only NLOS ranging takes place for anchors 303 and 304. The equation describing "RoomLinearCal" or rlc follows:

$$rlc_i^n = d_i^n + f_L(d_i^n, j) \quad (1)$$

where: d_i^n is the current (i) measured range between the roving node and anchor node n, f_L is the linear range corrections equation for room j.

The second calibration approach called "AllRoomLinearCal" produces the radial corrections for the total test area irrespectively of the room and therefore no distinction between LOS and NLOS conditions can be made. The corresponding calibration equation is:

$$arlc_i^n = d_i^n + f_l(d_i^n) \quad (2)$$

where: f_l is the linear range corrections equation for all rooms for anchor node n.

The third method refers to a bidimensional calibration fit that utilize the location of each calibration point based on its calibration value. In order to cover the total area of the test site the calibration values are interpolated using natural neighbor interpolation [15], which is based on the Voronoi tessellation method; hence, this calibration approach should be referred to as "VoronoiCal". For the area found outside the polygons defined by the calibration points a linear extrapolation is performed in order to extend the Voronoi calibration values.

$$vc_i^n = d_i^n + f_v(x_i^n, y_i^n) \quad (3)$$

where: f_v is the bidimensional range corrections equation for the moving node's position (x_i,y_i) and for anchor node n .

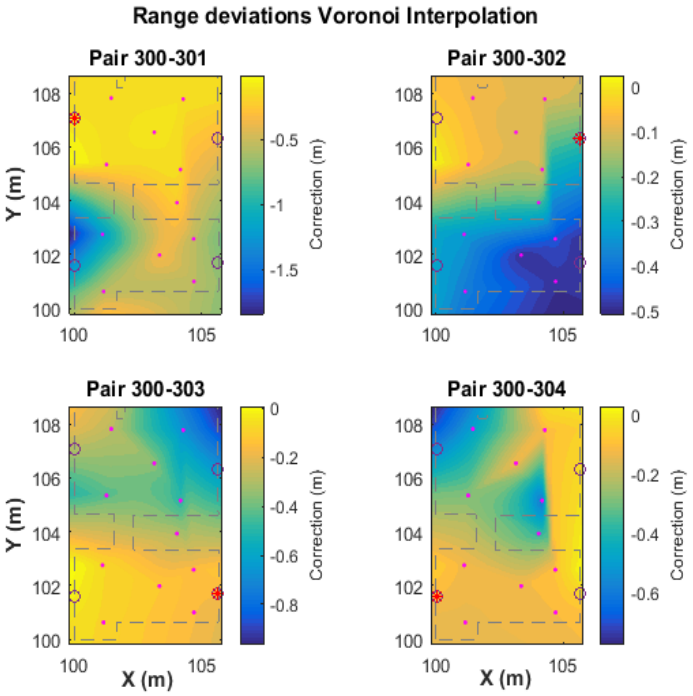

Fig. 7. Bidimensional interpolated range error Voronoi surfaces for the different UWB pairs

This method is preferred as it is expected to describe the variations in the calibration values either generated due to a change in the inter-node distance or due to the effect of NLOS ranging through various materials. Fig. 7 shows the results of "VoronoiCal" method. The plots of Fig. 7 indicate an apparent increase of the calibration values for NLOS areas. Another remark that relates to the values generated by the spatial extrapolation and especially for the right-most area of Room 1 for pair 300-302, is an irregular behavior that most likely relates to the extreme values found in the right-most area of Room 2 and the slight offset (towards right) of C7 and C10 with respect to locations of points C2 and C5.

B. Static ranges validation

In order to evaluate the efficiency of the three calibration methods, the range measurements collected for the validation points are extracted before performing any calibration and after implementing each calibration correction values. The output of the data for point V1 is shown in Fig. 8 in the form of histograms along with the generated "EPDF max" values for each method and the reference distance described by the vertical lines presenting an improvement in comparison with the uncalibrated values.

The diagram shown in Fig. 9 summarizes the performance of all validation points for each calibration method through reporting the mean deviation from the reference distance and its standard deviation for all UWB pairs. An expected improvement is apparent with all three methods compared to the "NoCalib" results. Moreover, differences in the performance between methods are recognized. In summary, the "AllRoomLinearCal" technique offers the minimum improvement while the performance of "VoronoiCal" proves to be marginally better compared to "RoomLinearCal" based on the smaller discrepancies between UWB pairs. Overall, the improvement compared to the "NoCalib" results ranges from 32% to 86%.

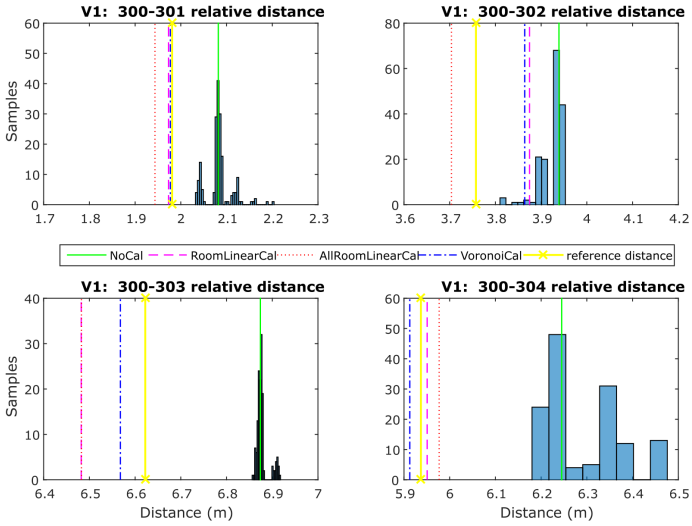

Fig. 8. Ranges histograms along with calibrated "EPDF max" values for the different calibration methods at point V1

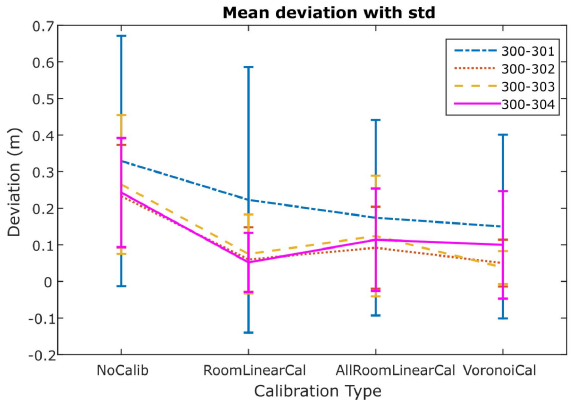

Fig. 9. Mean deviation per calibration method for all validation points along with the corresponding standard deviation

C. Trajectory validation

The kinematic positioning employs lateration using the measured ranges from the anchors of known coordinates. The position of the mobile node is estimated through a six-state [x, x', y, y', z, z'] constant velocity Extended Kalman Filter. While the current experimental set up yields a bidimensional problem, the inclusion the z values in the state vector allows the compensation of a small level difference between the two rooms. The noise of range measurements is defined by the error value reported by the UWB module for each measurement. The examination of the reported range errors against the estimated standard deviation of the ranging samples

leads to the need for a scaling factor of the reported error. Based on the relation between the reported LED values with the corresponding accuracy, an empirical scaling tactic is engaged during trajectory estimation as described by (4).

$$n(i) = \begin{cases} err_i^r * 5\ , & 7 < f_i^{LED} < 10 \\ err_i^r * 10, & 10 < f_i^{LED} \end{cases} \quad (4)$$

where: *n(i)* is the measurement noise implemented for sample *i*, err_i^r is the range error reported for sample *i* and f_i^{LED} is he LED flag value reported for sample *i*.

The different calibration methods are examined separately through implementing the calibration values to the ranges during each EKF run and in a dynamic manner. For the case of linear calibrations, the range correction value is calculated based on the reported range while for the Voronoi calibration the corresponding value is calculated based on the last known position estimated using the EKF. Fig. 10 shows the results obtained. In order to facilitate comparisons, the reference travel path is overlaid on the estimated trajectories.

More specifically, the plots of Fig. 10 provide a graphical representation of the performance of each method. The user trajectory starts at the top-left corner of Room 1 and ends up at the bottom-right of Room 2. The short stop & go sections are evident in the vicinity of each travel path at those bits where clouds of points (blue dots) are generated while the linear segments of the trajectory connect these clouds.

As far as the "NoCal" trajectory is concerned, the general pattern of the trajectory follows the designed path, however major deviations from the truth are evident. A constant offset as well as sections that appear to cross the walls of the laboratory generated by inaccurate range measurements amplify the need of calibrating the UWB ranges. The results for the "RoomLinerCal" method present a large improvement with the majority of the trajectory to coincide with the true path as well a closer concentration of the stop & go sections around the true points. Regarding the "AllRoomLinearCal" trajectory performance, the improvement compared to the "NoCal" method is also remarkable with the total of the points to closely follow the true path. It is noted that no points cross the wall limits however larger deviations compared to "RoomLinearCal" appear. For the trajectory generated with the "VoronoiCal" method the overall improvement appears to surpass the rest of the calibration methods. The trajectory is more stable and lies closer to the true path with one exception during the corridor pass where all the calibration methods present a weakness. This weakness is most probably the result of missing calibration points at boundary areas such as narrow passes between rooms with an unstable RF behavior. In this occasion, the corridor area calibration is produced with interpolated data, which effectively lack the necessary resolution required for boundary conditions.

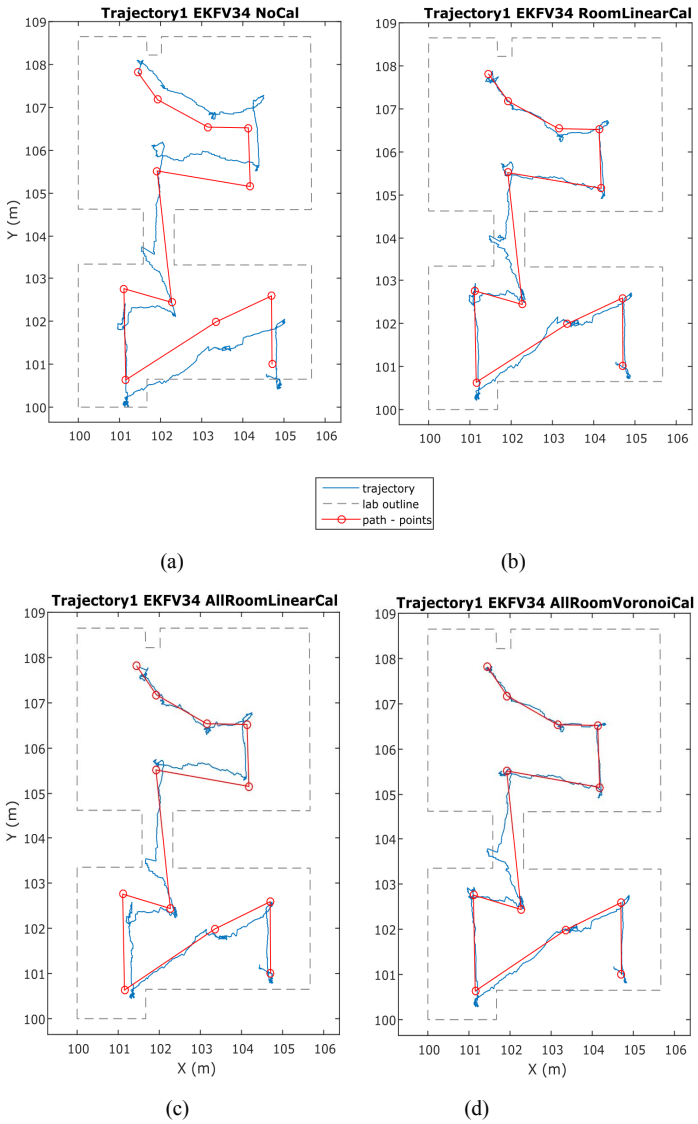

Fig. 10. Generated kinematic trajectories using the different calibration methods

Overall, the implementation of all the calibration methods improved the mobile node positioning with the "VoronoiCal" providing the best performance. The evaluation of the methods is summarized in Table 1 where the horizontal trueness values in terms of mean value, standard deviation and max value for each method are reported.

TABLE I. TRAJECTORY CALIBRATION METHODS STATISTICS

	Trueness (m)		
	mean	***sd***	***max***
No Calibration	0.35	0.20	0.85
Room Linear	0.13	0.10	0.62
All Room Linear	0.13	0.08	0.49
Voronoi Calibration	0.09	0.09	0.69

VI. CONLUSIONS

Indoor pedestrian positioning based on range lateration techniques is examined in this study. Raw UWB ranges suffer systematic errors in the form of bias for each ranging conversation. The elimination of this bias is attempted through collecting UWB ranges at known internodal distances between surveyed calibration points. Three methods are implemented here for generating the respective calibration models.

In order to evaluate the calibration models, raw and calibrated ranges collected at validation points of known locations are compared with the corresponding reference distances. The radial (1-dimensional) calibration methods suggest and improvement of the order of 32-78% compared to the performance of the uncalibrated raw ranges while the room-based radial calibration provides better adoption to the indoor environment. This is anticipated due to the room level grouping of the corrections which describe in reality the separate nature of correction values due the separate LOS and NLOS ranging conditions. The third calibration method using a bidimensional correction fitting process provides the most consistent and accurate results leading to an improvement of 86% compared to the uncalibrated ranges. Considering the spatially distributed nature of the range corrections this last method incorporates an appropriate empirical calibration model which is able to describe variations due to the indoor environments complex nature.

The final stage of the evaluation includes the dynamic implementation of the calibration methods for kinematic positioning. The calibrated ranges are fed to an EKF and the corresponding trajectories are produced. In agreement with the static tests results, the calibration methods suggest an improved performance for the kinematic trajectories. The bidimensional calibration method again provides the smallest error with a high repeatability with an instance of large deviation during a corridor pass.

This paper aims at proposing a general methodology for performing ad-hoc calibration for each indoor area of interest. Extracting global UWB ranging error models for indoor environments is proven to be a challenging task since unmodeled area-specific errors remain uncalibrated.

The main conclusion derived from the current study is that UWB ranging paired with the appropriate calibration methods is able to provide indoor positioning of high accuracy in the centimeter level. Evaluating the calibration methodology in different test areas with varying LOS/NLOS conditions can further support its generalization ability. An extension of the study would include the integration of additional positioning technologies able to provide continuous indoor positioning based on the high accuracy provided by UWB.

REFERENCES

[1] M. Kirkko-Jaakkola, S. Feng, Y. Xue, X. Zhang, S. Honkala, S. Söderholm, L. Ruotsalainen, W. Ochieng, H. Kuusniemi, “Effect of Antenna Location on GNSS Positioning for ITS Applications”. In Proceedings of the European Navigation Conference (ENC), Helsinki, Finland, 30 May–2 June 2016.

[2] V. Gikas and H. Perakis, “Rigorous Performance Evaluation of Smartphone GNSS/IMU Sensors for ITS Applications,” Sensors, vol. 16, no. 8, p. 1240, Aug. 2016.

[3] G. Chen, X. Meng, Y. Wang, Y. Zhang, P. Tian, and H. Yang, “Integrated WiFi/PDR/Smartphone Using an Unscented Kalman Filter Algorithm for 3D Indoor Localization,” Sensors, vol. 15, no. 9, pp. 24595–24614, Sep. 2015.

[4] Y. Bang, J. Kim, and K. Yu, “An Improved Map-Matching Technique Based on the Fréchet Distance Approach for Pedestrian Navigation Services,” Sensors, vol. 16, no. 10, p. 1768, Oct. 2016.

[5] G. Retscher and T. Tatschl, "Indoor positioning using Wi-Fi lateration — Comparison of two common range conversion models with two novel differential approaches," 2016 Fourth International Conference on Ubiquitous Positioning, Indoor Navigation and Location Based Services (UPINLBS), Shanghai, 2016, pp. 1-10.

[6] V. Gikas, H. Perakis, A. Kealy, G. Retscher, T. Mpimis, C. Antoniou, “Indoor Parking Facilities Management Based on RFID CoO Positioning in Combination with Wi–Fi and UWB”, FIG Working Week 2017, 29 May - 2 June 2017, Helsinki, Finland

[7] C. K. Toth, G. Jozkow; Z. Koppanyi, D. Grejner-Brzezinska, ”Positioning Slow-Moving Platforms by UWB Technology in GPS-Challenged Areas”, November 2017 Journal of Surveying Engineering 143(4):04017011

[8] R. Mautz, “Indoor Positioning Technologies”. Habilitation Thesis, ETH Zurich, Zurich, Switzerland, February 2012.

[9] S. Li, M. Hedley and I. B. Collings, "New Efficient Indoor Cooperative Localization Algorithm With Empirical Ranging Error Model," in IEEE Journal on Selected Areas in Communications, vol. 33, no. 7, pp. 1407-1417, July 2015. doi: 10.1109/JSAC.2015.2430273

[10] H. Jing, L. K. Bonenberg, J. Pinchin, C. Hill & T. Moore (2015) Detection of UWB ranging measurement quality for collaborative indoor positioning, Journal of Location Based Services, 9:4, 296-319, DOI: 10.1080/17489725.2015.1120359

[11] Z. Koppanyi, and C.K. Toth, Indoor Ultra-Wide Band Network Adjustment using Maximum Likelihood Estimation, ISPRS Ann. Photogramm. Remote Sens. Spatial Inf. Sci., II-1, 31-35, https://doi.org/10.5194/isprsannals-II-1-31-2014, 2014

[12] A. Ledergerber and R. D'Andrea, "Ultra-wideband range measurement model with Gaussian processes," 2017 IEEE Conference on Control Technology and Applications (CCTA), Mauna Lani, HI, 2017, pp. 1929-1934. doi: 10.1109/CCTA.2017.8062738

[13] D.Freedman and P. Z. Diaconis, “On the histogram as a density estimator: L2 theory” Zeitschrift für Wahrscheinlichkeitstheorie und Verwandte Gebiete (1981) 57:453

[14] Z. Koppanyi, C. Toth, D. Grejner-Brzezinska, G. Jóźków, “Performance Analysis of UWB Technology for Indoor Positioning”. Institute of Navigation International Technical Meeting 2014, ITM 2014.

[15] R. Sibson, A brief description of natural neighbor interpolation, in: V. Barnet (Ed.), Interpreting Multivariate Data, Wiley, Chichester, 1981, pp. 21–36